Pergamon

PII: S0960-0760(96)00015-5

J. Steroid Biochem. Molec. Biol. Vol. 58, No. 1, pp. 45–61, 1996

0960-0760/96 $15.00 + 0.00

Footprint Analysis of Estrogen Receptor Binding to Adjacent Estrogen Response Elements

Mark D. Driscoll, Carolyn M. Klinge,* Russell Hilf and Robert A. Bambara

Department of Biochemistry and the Cancer Center, The University of Rochester School of Medicine and Dentistry Rochester, NY 14642, U.S.A.

Quantitative DNase I footprinting assays were employed to simultaneously measure the amount of estrogen receptor (ER) bound to each site in constructs containing multiple estrogen response elements (EREs). These assays revealed identical, high affinity ER–ERE binding, K_d of approximately 0.25 nM, for estradiol-liganded ER (E_2–ER), 4-hydroxytamoxifen liganded ER (4-OHT-ER), tamoxifen aziridine liganded ER (TAz-ER), and unliganded dimeric ER, for each ERE in constructs containing up to four tandem EREs. Increasing concentrations of ER resulted in the same pattern of occupancy for each ERE, whether or not the site was located near other EREs. Similarly, the presence or absence of E_2, 4-OHT, or TAz ligand did not change ER–ERE interaction. Since activated ER–ERE binding affinity is identical, whether ER is liganded or unliganded, ligand cannot regulate ER–ERE binding affinity. These results support the hypothesis that ligand-dependent conformational changes primarily determine how ER interacts with components of the transcription initiation complex that mediate gene transactivation.

In addition, footprint assays revealed that, following ER binding, an AT-rich site adjacent to the ERE becomes hypersensitive to DNase I digestion. This sequence may be easily or intrinsically bent, assisting in recruiting ER to ERE sites. Copyright © 1996 Elsevier Science Ltd.

J. Steroid Biochem. Molec. Biol., Vol. 58, No. 1, pp. 45–61, 1996

INTRODUCTION

Estrogen receptor (ER) is a member of the superfamily of nuclear receptors that bind to specific DNA sequences. This superfamily includes receptors for steroid hormones, thyroid hormones, retinoids, and orphan receptors, for which no ligand is known. Ligand binding is thought to activate ER by initiating a series of events, which may include phosphorylation and dimerization, that enable ER to bind to estrogen response elements (EREs) found in the regulatory regions of estrogen responsive genes. The sequence of all known EREs is based on a perfect inverted repeat, 5'-GGTCAnnnTGACC-3'. However, many naturally occurring EREs vary from this core consensus sequence. The exact mechanism responsible for changes in gene transcription mediated by ER–ERE interaction is poorly understood. Transcription levels may be influenced by ER ligand, the affinity of ER–ERE interactions, by ER interaction with other transcription factors, by properties of DNA sequences flanking EREs, and by cooperative interactions between ERs bound to multiple ERE sites [1–3].

We recently examined the binding of E_2–ER to plasmid constructs containing from one to four tandem copies of a 38 base pair ERE consensus sequence [4]. These consensus sequences contain an AT-rich region that enhances ER–ERE affinity [5]. Equilibrium E_2–ER–ERE binding experiments yielded convex Scatchard plots and Hill coefficients greater than 1.5 for constructs containing three or four tandem consensus EREs, suggesting cooperative E_2–ER binding. In some cases, cooperative DNA binding may promote synergistic activation of transcription initiation [6–12]. The conditions that could promote cooperative ER binding

*Correspondence to: M. Klinge, Department of Biochemistry, Box 607, University of Rochester Medical Center, 601 Elmwood Avenue, Rochester, NY 14642, U.S.A.
Received 9 Jun. 1995; accepted 8 Dec. 1995.

to ERE sites remain poorly understood, however, and are the subject of the work presented here.

Antiestrogens have been used to study the properties of ER in the laboratory, and to treat breast cancer in a clinical setting. The triphenolic antiestrogen tamoxifen (TAM) is widely used in the treatment of women with advanced breast cancer or as an adjuvant, although its exact mechanism of action is unknown [13]. Depending on the tissues and species, TAM can display partial agonist as well as antagonist activity. Trans-4-hydroxytamoxifen (4-OHT), an active metabolite of TAM [14], binds ER with a 3-fold higher affinity than that of E_2 [15]. Although 4-0HT appears to bind to the same ER site as E_2 [16], a study of ER mutants identified amino acids in the hormone binding domain that interact differently with 4-0HT and E_2 [17]. Tamoxifen aziridine (TAz), an analog modified with a reactive aziridine moiety, binds covalently to ER in the ligand binding domain. The TAz–ER complex has the same sedimentation behavior on sucrose gradients as E_2–ER [18]. TAM, 4-OHT, and TAz induce mixed agonist and antagonist activities depending on the promoter and cell type. They are classified as Type I antagonists, because they impair transcriptional activation without blocking DNA binding [3].

The effect of ER on the transcription of estrogen responsive genes is determined by ligand. Several studies have suggested that the conformation of antiestrogen-liganded ER (AER) differs from that of E_2–ER [19–21]. Others have reported that the AER–ERE complex is altered in structure compared to the E_2–ER–ERE complex. Specific conformational changes in ER induced by ligand may be the mechanism by which estrogens and antiestrogens regulate transcription ([22, 23] reviewed in [1]).

If cooperative binding of ER to multiple EREs is stimulated by E_2, perhaps antiestrogens, such as TAM, prevent activation of estrogen responsive genes by interfering with ER–ER interactions. A series of experiments that measured association of 4-OHT liganded ER (4-OHT-ER) with ERE constructs containing one to four tandem 38 bp consensus EREs (Table 1) found no apparent cooperative ER binding, as indicated by linear Scatchard plots and Hill coefficients of ~ 1.0 [24]. These observations suggested a mechanism for the different transcriptional effects of ER induced by E_2 vs. 4-OHT, where E_2 was able to promote stabilizing ER–ER interactions leading to synergistic upregulation of transcription, but 4-OHT was not.

In this report, we investigated how the presence of multiple consensus EREs affected the binding of E_2–ER, 4-OHT-ER, TAz–ER, and unliganded, dimeric ER to EREs. Dissociation rates of E_2–ER and 4-OHT-ER from EREs were compared using nitrocellulose filter binding and gel mobility shift assays. If E_2 stimulated cooperative binding of ER by stabilizing protein–protein interactions directly, then the absence of 4-0HT–ER–ERE cooperative stabilization would predict a comparatively faster dissociation rate. DNase I footprinting experiments measuring the affinity of E_2–ER, TAz–ER, 4-OHT–ER, and unliganded ER for each of the sites in our ERE constructs allowed us to determine the effects of ligand and multiple tandem EREs on the affinity of ER–ERE interactions. We found that all ERE sites in the constructs we tested were occupied in an identical fashion, regardless of the ligand or the proximity of additional ERE sites.

EXPERIMENTAL

Preparation of ERE containing plasmids

DNA constructs containing ERE consensus sequences $(ERE)_1$, $(ERE)_2$, $(ERE)_3$, or $(ERE)_4$ (Table 1)

Table 1. *Sequences of ERE containing oligonucleotides*

A. Consensus ERE $(ERE)_1$

Inverted repeat — AT Rich Region

5'-CCA**GGTCA**GAG**TGACC**TGAGCTAAAATAACACATTCAG-3'

B. $(ERE)_{0.5}$

Half Inverted Repeat — AT Rich Region

5'-CCA**GGTCA**GAGCATTTCGAGCTAAAATAACACATTCAG-3'

C. $(ERE)_{AT}$

Inverted Repeat — AT Rich Region

TCA**GGTCA**GAG**TGACC**TGAGCTAAAATAACACATTCA-

AT Rich Region

GCTAGCACTGACGCTAGCGAGCTAAAATAACACATTC-

Inverted Repeat — AT Rich Region

AGCCA**GGTCA**GAG**TGACC**TGAGCTAAAATAACACATTCAA-3'

All oligonucleotides were cloned into the plasmid pGEM-7Zf(+) as described in Experimental. Half sequences of inverted repeats are in bold. The location of the AT-rich region is indicated above the sequence. $(ERE)_2$, $(ERE)_3$, $(ERE)_4$, and $(ERE)_8$ are 2, 3, 4 and 8 direct, head-to-tail, tandem repeats of the $(ERE)_1$ consensus sequence, respectively.

were cloned into the *Sma* I site of the plasmid pGEM-7Zf(+) (Promega, Madison, WI), as described previously [4]. Plasmid DNA was purified from JM 109 *E. coli* (Promega) using Qiagen tip-2500 columns (Qiagen Inc., Chatsworth, CA).

Preparation of ER

Partially purified ER was prepared from calf uteri as described previously [4, 24, 25]. Unliganded ER used in DNase I footprinting experiments was purified by ammonium sulfate precipitation followed by desalting on a G-25 Sephadex (Sigma, St. Louis, MO) spin column equilibrated with TDPK 111 (40 mM Tris–HCl, pH 7.5, 1 mM DTT, 0.5 mM PMSF, 111 mM KCl).

ER was liganded with either 17β-[2,4,6,7,16,17-^{3}H] E_2 (142 Ci/mmol NEN, DuPont, Boston, MA), Z-4[*N*-methy-^{3}H] 4-OHT (81.1 Ci/mmol, NEN, DuPont, Boston, MA), or [ring-^{3}H]tamoxifen aziridine (23 Ci/mmol, Amersham, Arlington Heights, IL). The ammonium sulfate precipitated uterine cytosol was subjected to heparin agarose affinity chromatography (Affi-Gel Heparin, BioRad, Richmond, CA). For some experiments ER was purified further, to over 90% of total protein, by sequence-specific DNA affinity chromatography [26]. For footprinting assays, ER containing fractions pooled from columns were diluted to 111 mM KCl with buffer A (10 mM Tris–HCl, pH 8.0, 5 mM $MgCl_2$, 1 mM $CaCl_2$, 2 mM DTT, 50 μg/ml BSA, 2 μg/ml sonicated salmon sperm DNA). The pooled ER was diluted further with buffer A containing 111 mM KCl to obtain approximately 5 nM ER. All concentrations of ER refer to the amount of dimeric ER complex. Final concentrations of ER were determined by hydroxyapatite (HAP) assay.

Nitrocellulose filter binding assay comparing dissociation rates of E_2ER and 4-OHT-ER from $(ERE)_3$ and $(ERE)_4$

The pGEM-7Zf(+) plasmid DNA, with or without EREs, was linearized by *Eco*RI digestion and labeled by *E. coli* DNA polymerase I Klenow fragment incorporation of α[^{35}S]dATP (600 Ci/mmol, Amersham, Arlington Heights, IL) for use in nitrocellulose filter assays. For each experiment, ER was preincubated at 4°C with [^{35}S] plasmid, with or without $(ERE)_{1-4}$, for 2.5 h, when steady state binding was reached. At time zero, 550-fold excess unlabeled plasmid DNA containing eight copies of the consensus $(ERE)_1$ sequence $(ERE)_8$ was added as competitor. The samples were incubated at 22°C, and 80 μl aliquots were removed at regular intervals over the 3 h incubation. ER molecules that dissociated from EREs during the course of the assay were sequestered by the unlabeled $(ERE)_8$ competitor. The aliquots were applied to nitrocellulose filters (Schleicher and Schuell, Keene, NH; BA 85, 0.45 mm) which had been prewetted using 1 ml TDPK 100 (40 mM Tris–HCl, pH 7.5, 1 mM DTT, 0.5 mM PMSF, 100 mM KCl) and the specific binding of ER–ERE was followed over time. The binding of ER to [^{35}S]pGEM-7Zf(+) without ERE represented 'background' binding of ER to plasmid DNA. Specific binding was calculated by subtracting background from the amount of [^{35}S]pGEM-7Zf(+) containing ERE at each time point.

Gel mobility shift assay comparing dissociation rates of E_2–ER and 4-OHT-ER from EREs

pGEM-7Zf(+) plasmid containing ERE inserts was prepared for the gel mobility shift assays by digesting with *Eco*RI and *Bam*HI. ERE-containing fragments were purified by polyacrylamide gel electrophoresis, and electroeluted (UEA Electroelutor, International Biotechnologies, Inc., New Haven, CT). Purified ERE-containing fragments were labeled by *E. coli* DNA polymerase I Klenow fragment incorporation of α[^{32}P]dATP (400 Ci/mmol, Amersham, Arlington Heights, IL). Unincorporated nucleotides were removed by centrifugation through a G-50 Sephadex spin column equilibrated in TE buffer (10 mM Tris–HCl, 1 mM EDTA, pH 8.0).

For the gel shift dissociation experiments, each reaction contained 5 μg poly d(I–C) and 50 000 dpm (12.5 fmol) [^{32}P]ERE. The amount of E_2–ER or 4-OHT-ER added (approximately 125 fmol) was expected to saturate the available ERE sites. The ER–ERE mixture was allowed to reach equilibrium over 2.5 h at 4°C. After 30 min at 23°C, unlabeled competitor $(ERE)_8$ was added, and dissociation was followed for 3 h.

To determine the effect of 23°C incubation on the stability of the ER–ERE complexes, TE was added, instead of $(ERE)_8$, to one set of tubes in each experiment. After 3 h at 23°C, the samples were loaded onto a non-denaturing 5% polyacrylamide gel and electrophoresed at 4°C for 3 h. Autoradiography was performed at −80°C with an intensifying screen (DuPont Lightning Plus). The autoradiographs were quantitated using a model 400X computing densitometer (Molecular Dynamics, Sunnyvale, CA) linked to a Sun Microsystems SPARC Station 1 computer.

DNase I footprint assay of the affinity of ER–ERE binding

The ERE-containing pGEM-7Zf(+) plasmid DNA used in footprint assays was digested with *Eae*I, followed by treatment with calf intestinal phosphatase (New England Biolabs, Beverly, MA). The fragments were separated on a 5% acrylamide gel, and the ERE containing fragment was electroeluted. The DNA was digested further with *Pvu*II, resulting in a 353 bp fragment containing the ERE sites, and a 10 bp fragment. The 3' end labeling was carried out using α[^{32}P]ATP (6000 Ci/mmol, Amersham) and dCTP, whereas 5' end labeling was accomplished using T4 polynucleotide kinase and γ[^{32}P]ATP (6000 Ci/mmol,

Amersham). Unincorporated nucleotides and the 10 bp fragment left after *Pvu*II digestion were removed by passing the DNA over a 1 ml G-50 Sephadex spin column equilibrated in water. The DNA was sequenced by the method of Maxam–Gilbert [27], and sequencing reactions were analyzed alongside footprinting reactions.

DNase I footprinting reactions contained 1.5 μg poly d(I–C) (Midland Certified Reagent Co., Midland, TX), 20 000 dpm [^{32}P]ERE (approximately 1 fmol), ER, and buffer A containing 111 mM KCl to a final reaction volume of 158 μl. ER–ERE binding was allowed to equilibrate for 3 h at 4°C. The tubes were then incubated at 25°C for 30 min. DNase I (Promega) (0.625 units) was added to each tube, and the tubes were incubated at 25°C for 2 min 40 s. Digestion was terminated by the addition of 80 μl DNase I stop solution (20 mM Tris–HCl, pH 8.0, 250 mM NaCl, 20 mM EDTA, 0.5% SDS, 50 μg/ml sonicated salmon sperm DNA, 125 μg/ml proteinase K), and the mixtures were incubated at 44°C for 1 h. The DNA was ethanol precipitated, washed twice with 70% ethanol, dried, and resuspended in 5 μl formamide loading buffer [98% deionized formamide (Sigma), 10 mM EDTA, pH 8.0, 0.025% xylene cyanole, 0.025% Bromophenol Blue]. Samples were heated to 90°C for 5 min, quenched on wet ice, and loaded onto a denaturing 15% polyacrylamide gel. Samples were electrophoresed at 1900 V for 7 h. The gels were fixed for 30 min in a solution of 5% acetic acid and 5% methanol, and dried under vacuum at 70°C. Autoradiography was typically performed over 2 days at −80°C with Kodak X-OMAT AR film and an intensifying screen (DuPont Lightning Plus). The autoradiographs were quantitated using a model 400X computing densitometer (Molecular Dynamics, Sunnyvale, CA) connected to a Sun Microsystems SPARC Station 1 computer.

Quantitative DNase I footprinting

The DNase I footprint procedure presented here was an adaptation of the method of Brenowitz *et al.* [28]. For measurements of ER–ERE binding constants to be accurate, the footprinting reactions have to be performed at equilibrium. Footprinting reactions measuring ER–ERE binding at low (30 pM) and high (1.2 nM) concentrations of ER reached equilibrium by 60 min at 4°C and remained stable for 19 h (data not shown). Additionally, experiments using a range of DNase I concentrations yielded identical results, demonstrating that DNase I did not interfere with ER–ERE equilibrium (data not shown).

Determination of fractional saturation curves used unprotected areas in each lane as standards, both above and below the protected regions. DNase I exposure was adjusted so that digestion was uniform in the areas of interest, such that the fractional saturation curve ranged between 0 and 1.

Fractional saturation, defined by Brenowitz *et al.* [28] is expressed as

$$Y = 1 - ([Dn,site/Dn,Std]/[Dr,Site/Dr,Std]),$$

where *Dn,site* is the sum of the OD in a footprint site in lane n, and *Dn,Std* indicates the total OD for the standard in lane n. *Dr* is the reference lane where no ER is added.

The affinity constant, K_d, is closely approximated by the [ER] at 0.5 fractional saturation. This is shown by the following:

$$[ERfree] + [EREfree] \rightarrow [ER - ERE]$$

$$So, \quad K_d = [ERfree][EREfree]/[ER - ERE].$$

$$At\ Y = 0.5,\ [EREfree] = [ER - ERE] = 1/2[ERE],$$

$$so, \quad K_d = [ERfree].$$

$$Since\ [ERfree] = [ERTotal] - [ER - ERE]$$

$$and\ [ER - ERE] = 1/2[ERE],$$

$$[ERfree] = [ERTotal] - 1/2[ERE].$$

$$Finally, \quad K_d = [ERTotal] - 1/2[ERE].$$

This equation indicates that [ER] at 50% fractional saturation closely approximates K_d when the [ERE] is significantly below K_d. For the experiments reported here, the [ERE] was approximately 5 pM, 40-fold below the ER–ERE K_d.

RESULTS

DNase I footprint of ER

DNase I footprinting was used to compare the extent of the $(ERE)_1$ sequence protected by liganded and unliganded ER (Fig. 1). The heparin agarose purified E_2–ER footprint of $(ERE)_1$ covered a 22 bp region, centered on the ERE palindrome (E, lane 2). Identical footprints were obtained for 4-OHT-ER (T, lane 3), TAz–ER (Z, Lane 4), and E_2–ER purified by ERE–Sepharose affinity chromatography (E_a, lane 5). In the absence of ER, no footprint was detected (Lane 6). Differences in footprint intensity reflect the different concentrations of ER used in the experiment. The identical size of the protected regions reveals that 4-OHT-ER and TAz–ER protect the same area surrounding this ERE as E_2–ER. Unliganded ER also contacts the same 22 nucleotides (data not shown) as the liganded forms of ER, suggesting that changes induced by ligand binding exert little or no effect on how ER protects ERE sites. Additionally, the AT-rich region and other areas adjacent to the ERE showed no evidence of protection (data not shown). Likewise, when examining ER interaction with multiple tandem EREs, the region protected by ER was identical for all sites in $(ERE)_{1-4}$ (data not shown).

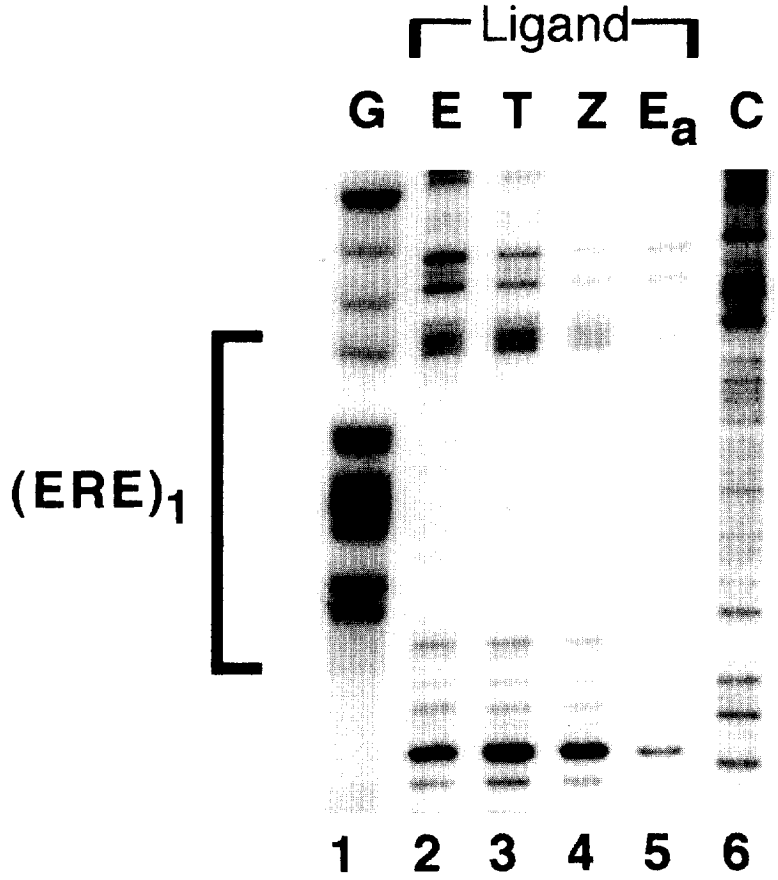

Fig. 1. DNase I footprint of liganded ER binding to $(ERE)_1$ Double stranded [^{32}P]$(ERE)_1$ and 1.5 μg poly d(I–C) was incubated with 4.43 nM E_2–ER (E, lane 2), 4.94 nM 4-OHT-ER (T, lane 3), 9.43 nM TAz-ER (Z, lane 4), 1.16 mM ERE affinity purified E_2–ER (Ea, lane 5), or assay buffer as a control (C, lane 6). The mixtures in lanes 2–6 were treated with DNase I as described in Experimental. Lane 1 (G) contains [^{32}P]$(ERE)_1$ sequenced by the G-reaction of the method of Maxam–Gilbert. The ERE footprint site is indicated by brackets at the left of the figure.

ER–ERE affinity as measured by DNase I footprint assay

ER binding to $(ERE)_1$ was the standard to which ER binding to $(ERE)_2$, $(ERE)_3$, and $(ERE)_4$ was compared. If ER–ER interactions enhance binding to ERE sites, increased affinity for these sites in the context of multiple EREs when compared to $(ERE)_1$ would be predicted. If ER bound to each ERE in $(ERE)_2$, $(ERE)_3$, and $(ERE)_4$ in an independent, non-cooperative manner, then the saturation curves for each site in each construct should be identical to the $(ERE)_1$ saturation curve, yielding identical values for K_d.

DNase I footprinting of E_2–ER was performed for each of the constructs $(ERE)_{1-4}$ (Fig. 2A–D). The concentration of receptor was varied so that the fractional saturation ranged from 0 (EREs unoccupied) to 1 (EREs fully occupied). Quantitation of the protected regions was performed as described in Experimental. The fractional saturation curves were graphed (Fig. 3A–D), and the K_d values were determined (Table 2). As expected, the affinity of ER (Table 2) for the 38 base pair consensus sequence was similar to that obtained by other methods [4, 29, 30]. In addition, the occupancy of each ERE site within each of the constructs responded similarly to increasing concentrations of E_2–ER. We observed no ligand- or ERE context-dependent changes in ER–ERE affinity. Thus, ER binds with the same affinity to EREs whether liganded with E_2, 4-OHT, TAz, or unliganded. ER also binds with identical affinity whether or not there are adjacent ERE binding sites.

DNase I footprinting was performed on two additional constructs. One of these was $(ERE)_{0.5}$ (Table 1), in which the right half of the ERE inverted repeat was changed from 5'-TGACC-3' to 5'-CATTT-3', leaving only an ERE half site. We observed no binding of E_2–ER to this ERE, even at E_2–ER concentrations as high as 20 nM. The second construct, ERE–AT (Table 1), contains two 38 base pair consensus EREs spaced seven helical turns apart. This arrangement duplicates the positioning of the first and third sites of the $(ERE)_3$ construct, where the EREs lie on the same face of the DNA helix. ERE–AT also contains an extra copy of the consensus AT-rich sequence between the two ERE sites. E_2–ER binding to this ERE displays cooperative parameters similar to those found for $(ERE)_3$ [5]. If interaction between ER

bound to the first and third sites of $(ERE)_3$ results in stabilization of ER–ERE binding, then increased ER–ERE affinity would be predicted. However, the affinity of E_2–ER for both ERE sites in ERE–AT was 0.20 ± 0.05 nM, indistinguishable from the affinity of ER for $(ERE)_1$. Thus, cooperative binding parameters determined previously for ERE–AT were not indicative of ER–ER interactions that stabilize ER–ERE binding.

Comparison of E_2–ER and 4-OHT–ER–ERE binding by gel mobility shift assay

The gel mobility shift assay was used to compare the effect of the ligands E_2 and 4-OHT on the rate of ER dissociation from various ERE constructs. In these experiments, the rate of ER dissociation was measured by following the gradual disappearance of the retarded ER–ERE complexes and the simultaneous appearance of free ERE DNA (Fig. 4A,B). In these assays, the amount of E_2–ER or 4-OHT–ER added was enough to fully saturate all available ERE sites. Because dissociation of ER from EREs at 4°C was very slow (data not shown), dissociation was measured at room temperature (23°C). To determine the effect of incubation at 23°C on the stability of the ER–ERE complex, TE alone was added, instead of $(ERE)_8$ competitor in TE, to one set of tubes. After 3 h at 23°C, gel electrophoresis was performed (Fig. 4A, lanes 1–8). The amount of E_2–ER or 4-OHT–ER–ERE complex present after incubation with TE at either 23°C or 4°C was the same (data not shown). These results indicate that the ER–ERE binding remains stable at 23°C over the 3 h time course of the dissociation assay.

The pattern of retarded ER–ERE bands was similar for both receptor ligands, although the 4-OHT–ER–

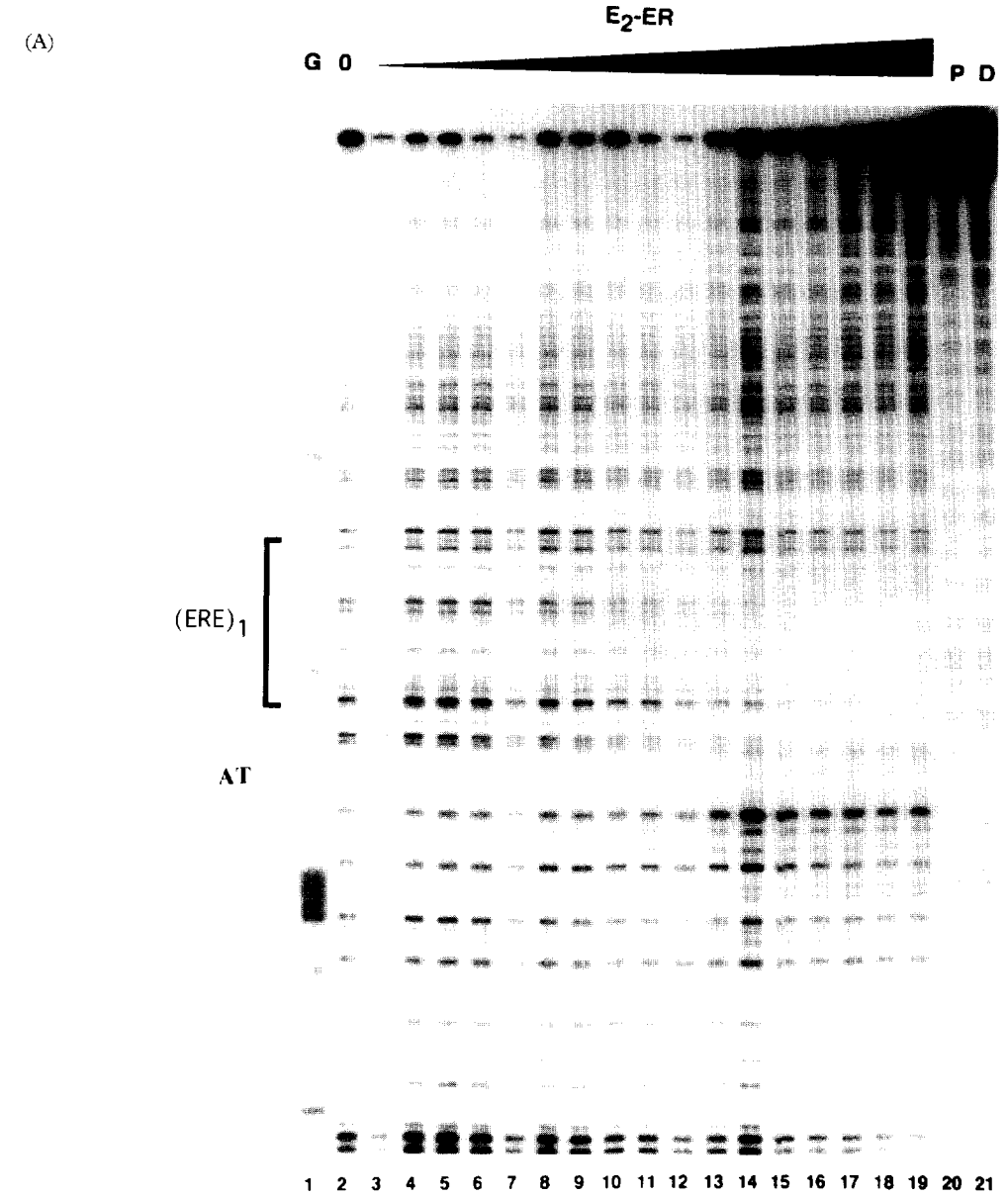

Fig. 2(A)—*caption on page 53*

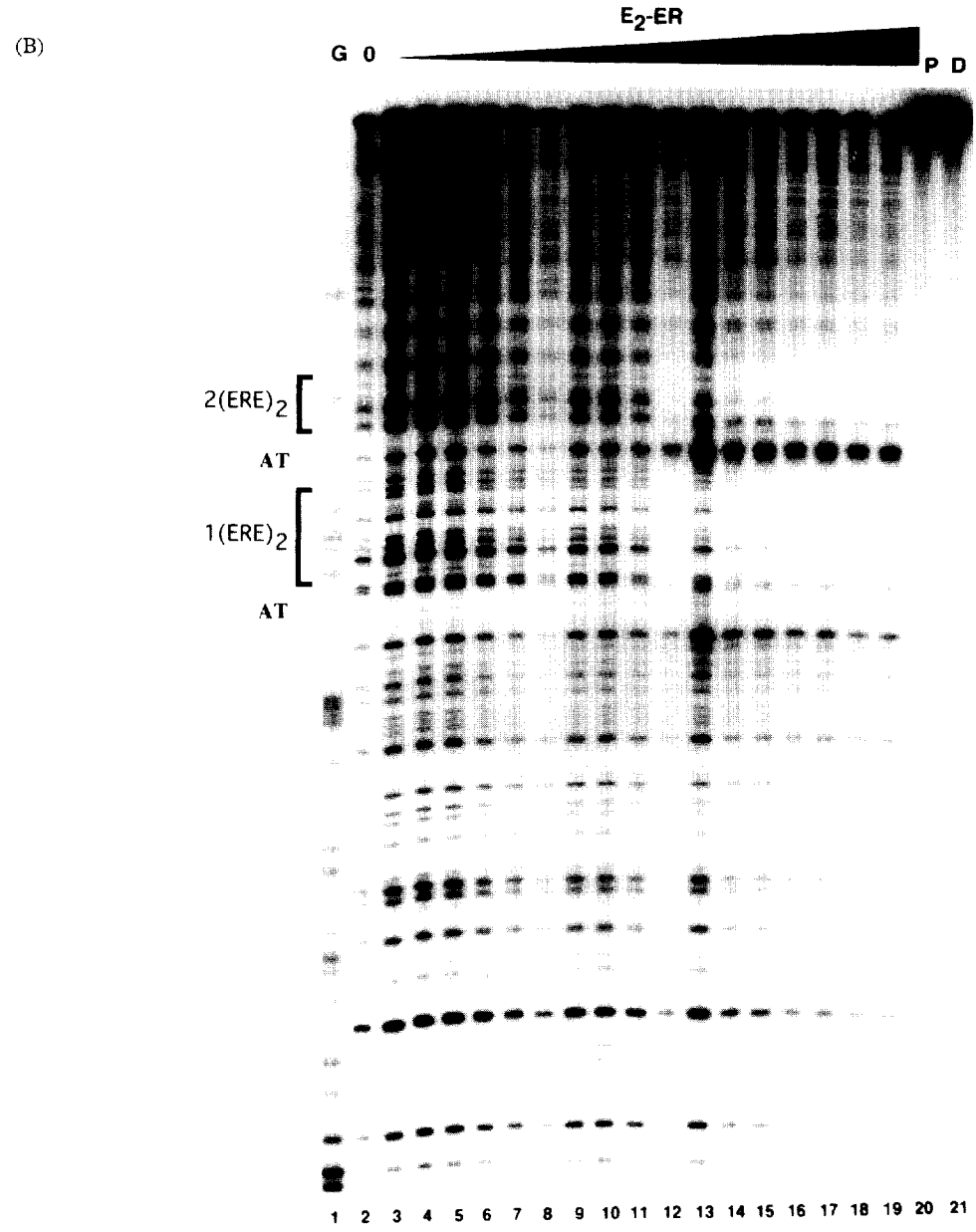

Fig. 2(B)—*caption on page 53*

ERE complexes appear to be slightly more retarded than the E_2–ER–ERE complexes. Interestingly, 4-OHT–ER appeared to have bound less $(ERE)_2$, $(ERE)_3$ and $(ERE)_4$ than E_2–ER, since more free ERE was detected in each lane containing 4-OHT–ER (Fig. 4A, B; compare E with T). Additionally, the stability of 4-OHT–ER binding to the $(ERE)_4$ construct is less than that of E_2–ER binding to the $(ERE)_4$ construct since, even in the absence of competitor ERE, a complex of 3 4-OHT–ER$(ERE)_4$ was detected (Fig. 4A, lane 8). In contrast, only the 4 ER–$(ERE)_4$ complex is detected when ER is liganded with E_2 (Fig. 4A, lane 4).

Both E_2–ER and 4-OHT–ER binding to $(ERE)_1$ resulted in the appearance of three retarded complexes (Fig. 4A, lanes 1 and 5). This observation is similar to those reported by others [30]. Multiple ER–$(ERE)_1$ complexes might result from differential phosphorylation of ER, or binding of other proteins to the ER–ERE complex [31].

Titration of E_2–ER and 4-OHT–ER concentrations from 0 to 200 fmol with a fixed concentration of $(ERE)_2$, $(ERE)_3$, or $(ERE)_4$ (20 fmol) showed that, at subsaturating concentrations of ER, complexes similar to those detected for $(ERE)_1$ were formed (data not shown). Although these complexes migrated slightly slower because of the larger size of the ERE-containing oligomer, their migration corresponds to one ER dimer bound to only one of the tandem EREs. Depending on the concentration of ER, $(ERE)_2$ formed bands corresponding to one ER dimer bound $(1(ERE)_2)$ or two ER dimers bound $(2(ERE)_2)$. Similar patterns were

obtained with $(ERE)_3$ or $(ERE)_4$, where each oligomer contained only one or two ER dimers bound at low ER concentrations. Additionally, $(ERE)_3$ and $(ERE)_4$ also formed complexes that contained three [in $(ERE)_3$ and $(ERE)_4$] or four [$(ERE)_4$ only] ER dimers bound as ER concentration was increased.

The various E_2- and 4-OHT–ER–ERE complexes described above were resistant to challenge by 100-fold excess non-specific competitor DNA, including salmon sperm DNA and poly d(I–C), but ER was sequestered by equivalent amounts of specific competitor $(ERE)_4$ (data not shown). Thus, ER–ERE binding is specific and requires high affinity ERE binding sites. To confirm that the retarded ER–ERE complexes contained ER, E_2–ER or 4-OHT–ER was incubated with ERE and H222, a monoclonal antibody raised against intact human ER [32]. Inclusion of this ER-specific antibody produced 'supershifted' antibody ER–ERE complexes, along with the disappearance of all ER–ERE complexes (data not shown). These results confirm the presence of ER in the retarded ER–ERE complexes.

ER–ERE stability as measured by gel mobility shift assay

To more accurately determine the rates of ER dissociation from ERE constructs, the amounts of free ERE appearing in gel shift assays (Fig. 4A,B) were quantitated by densitometric scanning (Fig. 5A–D). Quantitation of the amount of free ERE is a more accurate measure of the conditions at the time of sample loading than the amount of retarded complex, since dissociation of ER–ERE complexes may occur during electrophoresis [33]. The amount of free ERE present

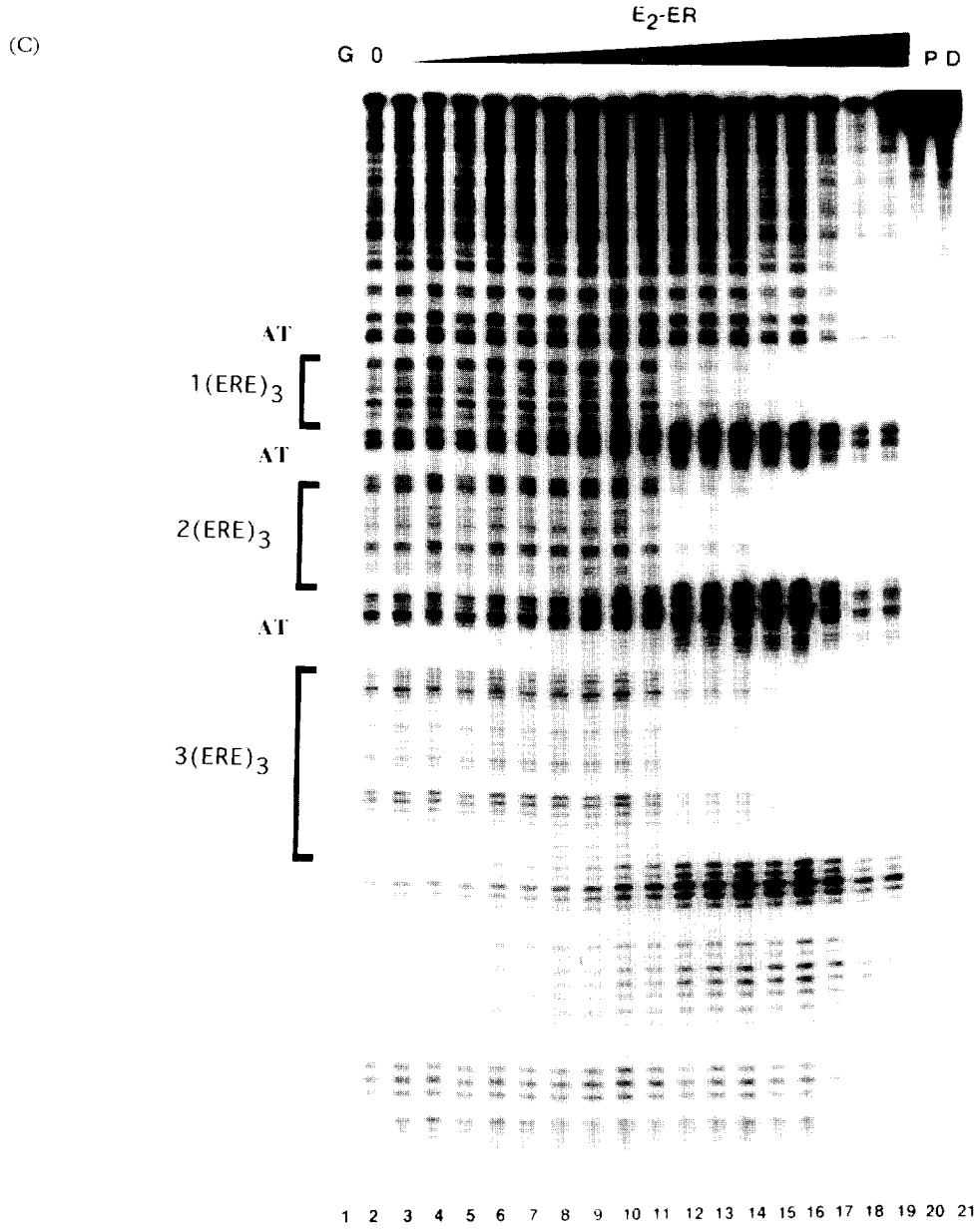

Fig. 2(C)—*caption opposite*

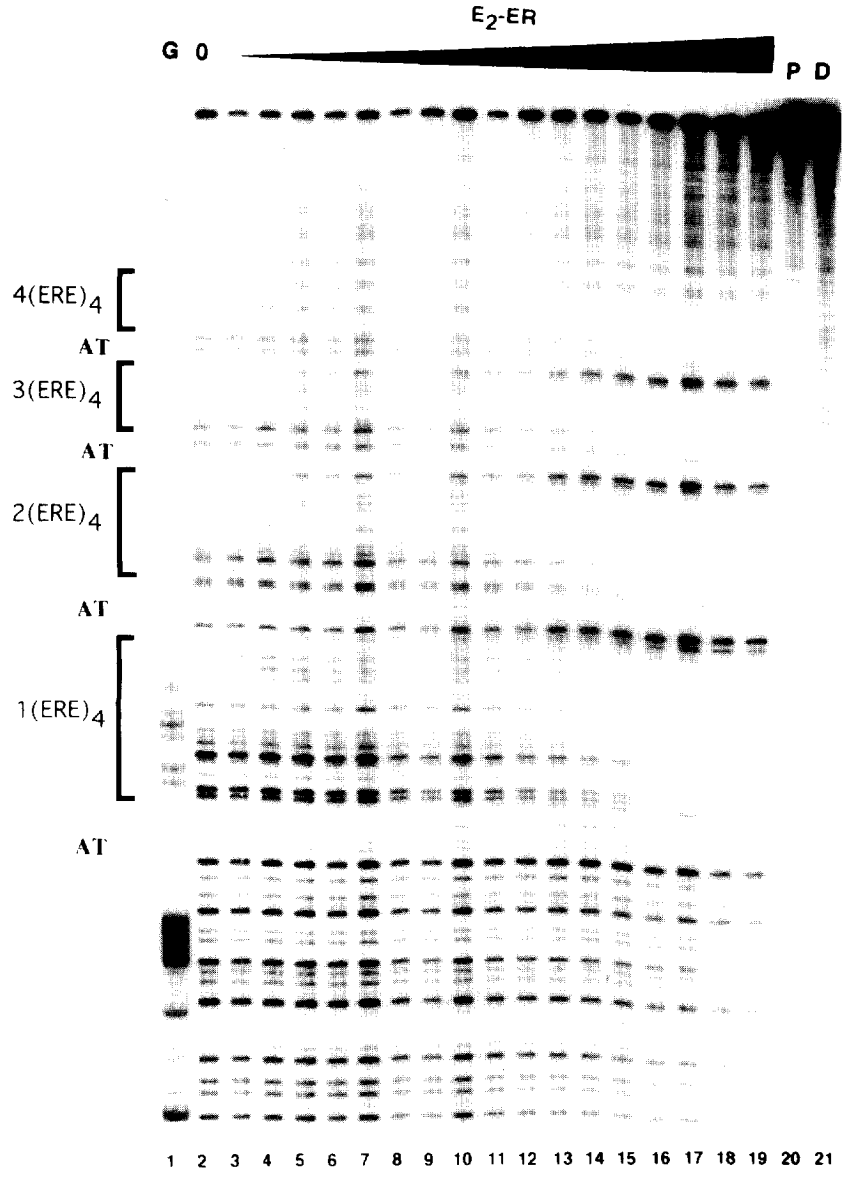

Fig. 2D

Fig. 2. Quantitative DNase I Footprints of $(ERE)_{1-4}$. (A), (B), (C) and (D) are DNase I footprints of $(ERE)_1$, $(ERE)_2$, $(ERE)_3$, and $(ERE)_4$, respectively. Lane numbers are indicated at the bottom of the gel. In each gel, lane 1, (G), contains ERE sequenced by the G-reaction of the method of Maxam–Gilbert. ERE footprint sites (brackets) and the location of the AT-rich regions (AT), are indicated at the left of the figure. One fmol of the appropriate ERE was incubated with 1.5 μg poly d(I–C) in lanes 2–19, and increasing amounts of E_2–ER were added to lanes 3–20. The mixture in lane 20 contained ER (P = protein control), whereas lane 21 received the equivalent volume of assay buffer (D = DNA control). Following incubation for 2.5 h at 0°C, the mixtures were warmed to 25°C. The mixtures in lanes 2–19 were then treated with DNase I. Lanes 20 and 21 received assay buffer instead of DNase I as described in Experimental.

in the band at the bottom of the gel is the amount of free ERE present when the sample was loaded onto the gel, and is not affected by dissociation during electrophoresis. Levels of retarded ER–ERE complex at 0 min for $(ERE)_3$ and $(ERE)_4$ (Fig. 4B, lanes 17–20) were lower than those of the controls in Fig. 4A, where no $(ERE)_8$ was added (lanes 3, 4, 7, 8). This probably reflects ER dissociation from ERE during the time required to load the gel, as well as during electrophoresis.

The amount of free $(ERE)_1$ appearing over the time course of the experiments was quantitated for lanes containing E_2–ER and 4-OHT–ER. (Fig. 5A). Similar amounts of free $(ERE)_1$ were observed in each case over 180 min. The slopes of the best fit lines, determined by linear regression, indicated that E_2–ER dissociated 1.07× faster than 4-OHT–ER. Thus, there was no detectable difference in dissociation rates between E_2–ER and 4-OHT–ER from $(ERE)_1$.

More free $(ERE)_2$ was seen at 0 min (Fig. 4A, lanes

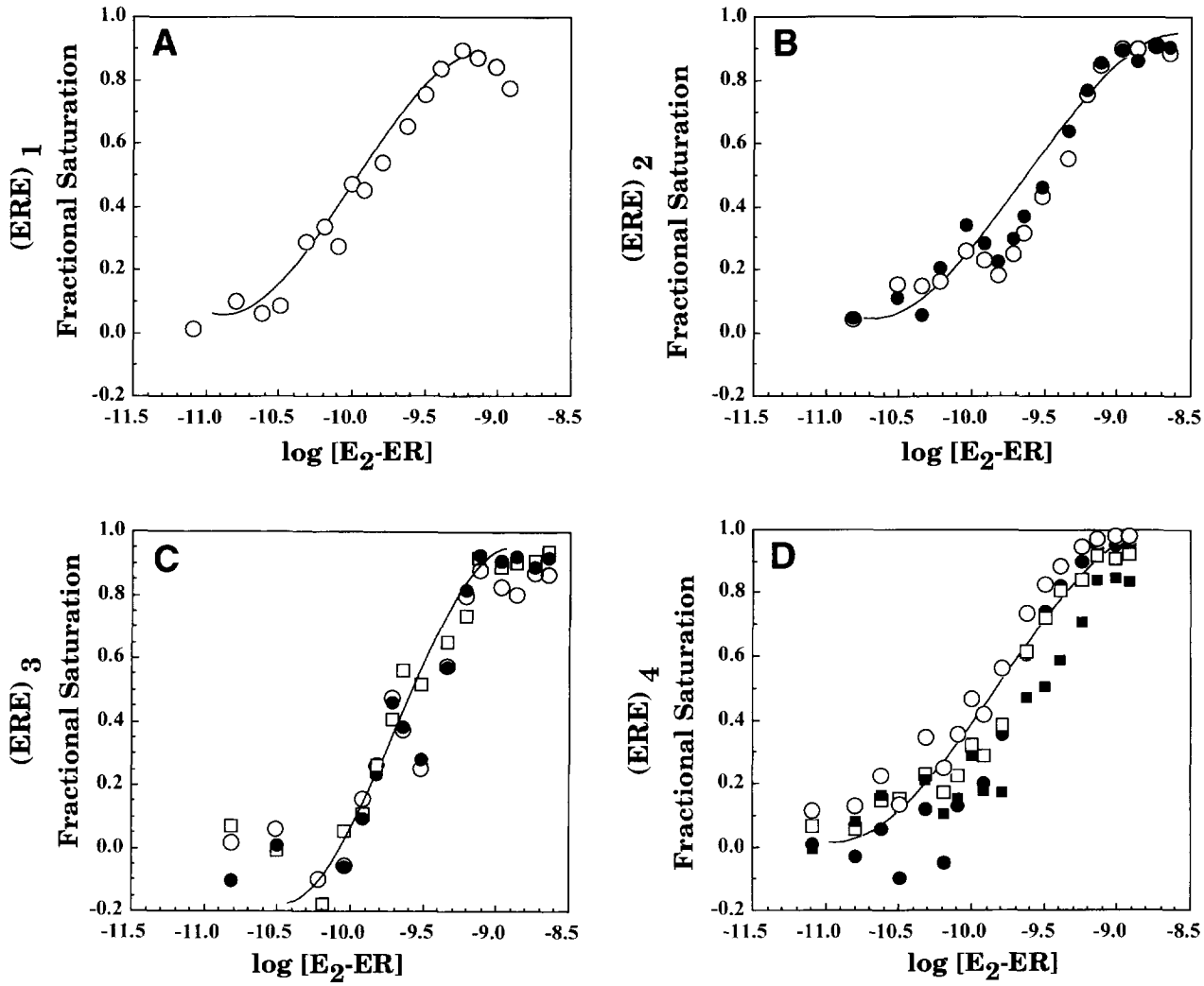

Fig. 3. Fractional saturation plots of E_2–ER–ERE footprints.The fractional saturation of footprints in Figs 2(A)–(D) were quantitated in Figs 3(A)–(D) as described in Experimental, and graphed. Open circles represent the first ERE site in each construct, closed circles the second, open squares the third, and closed squares the fourth. Lines were calculated by least square regression analysis. As [ER] increased, the fractional saturation increased from 0 (no footprint) to 1 (fully footprinted).

27 and 28) in lanes containing 4-OHT–ER than in lanes with E_2–ER, and this difference remained constant throughout the dissociation assay (Fig. 5B). As expected, the addition of competitor $(ERE)_8$ at time 0 led to increasing amounts of free $(ERE)_2$. Densitometric scanning of the amount of free $(ERE)_2$ (Fig. 5B) showed that the rate of increase in the amount of free $(ERE)_2$ with time was comparable for 4-OHT–ER and E_2–ER, despite the curvilinear appearance of the graph. Hence, the rates of ER dissociation from $(ERE)_2$ are similar for ER bound with either ligand.

Results for $(ERE)_3$, as with $(ERE)_2$, showed a ligand-dependent difference in the initial amount of free ERE (Fig. 4B, lanes 17 and 18), Following the

Table 2. Affinity of E_2–ER, 4-OHT-ER, TAz–ER and unliganded ER for $(ERE)_{1-4}$

Ligand	n^a	$(ERE)_1^b$	n^a	$(ERE)_2^b$	n^a	$(ERE)_3^b$	n^a	$(ERE)_4^b$
E_2	4	0.25 ± 0.03	4	0.29 ± 0.05	5	0.23 ± 0.06	4	0.21 ± 0.05
4-OHT	3	0.33 ± 0.09	3	0.20 ± 0.05	3	0.20 ± 0.01	3	0.16 ± 0.07
TAz	5	0.24 ± 0.04	4	0.27 ± 0.03	3	0.25 ± 0.03	3	0.35 ± 0.08
None	3	0.16 ± 0.05	3	0.25 ± 0.08	2	0.31 ± 0.15	3	0.28 ± 0.08

The K_d values for ER–ERE binding were obtained from fractional saturation plots, as described in Experimental, using a fixed concentration of ERE and increasing concentrations of [^{3}H]E_2–ER, [^{3}H]4-OHT-ER, [^{3}H]TAz–ER, or unliganded ER.[a]n = number of experiments.[b]The K_d in in nM, plus or minus the standard error of the mean (SEM). Constructs containing multiple ERE sites were found to have identical K_d values for each site, so only a single value is shown.

addition of $(ERE)_8$, free $(ERE)_3$ appeared at similar rates from complexes containing 4-OHT–ER or E_2–ER (Fig. 5C). Consequently, best fit lines through the data in Fig. 5C show that the rates of 4-OHT–ER and E_2–ER dissociation were comparable.

In contrast to the results for $(ERE)_1$, $(ERE)_2$, and $(ERE)_3$, a difference in the rate of appearance of free ERE was observed for $(ERE)_4$. Quantitation of free $(ERE)_4$ is shown in Fig. 5D. At 0 min, the amount of free ERE for 4-OHT–ER (Fig. 4B, lane 20) was again higher than for E_2–ER (Fig. 4B, lane 19). The difference in the slopes of the lines showed that 4-OHT–ER dissociated from $(ERE)_4$ 2.6× faster than E_2–ER. This small difference in dissociation rates contrasts with the results of both the nitrocellulose filter dissociation assay and the DNase I footprint assay, where identical kinetics were measured for both liganded forms of ER.

ER dissociation as measured by nitrocellulose filter assay

Nitrocellulose filter assays [8] were employed as an alternative method to measure the effect of ligand on ER dissociation from EREs. As with the gel shift assay, we expected that cooperative binding should stabilize E_2–ER–ERE interactions, resulting in slower dissociation rates for E_2–ER from $(ERE)_3$ and $(ERE)_4$ compared to 4-OHT–ER, which did not display cooperative binding.

In each experiment, ERE was incubated with saturating levels of ER to equilibrium. Then, 550-fold excess ERE ($(ERE)_8$) was added as competitor, and the amount of specific binding of ER–ERE was followed over time. After the addition of competitor ERE, the amount of [^{35}S]ERE specifically bound to [^{3}H]E_2–ER or [^{3}H]4-0HT–ER decreased. Each experiment measured dissociation from plasmid DNA containing either $(ERE)_3$, $(ERE)_4$, or lacking an ERE insert. The amount

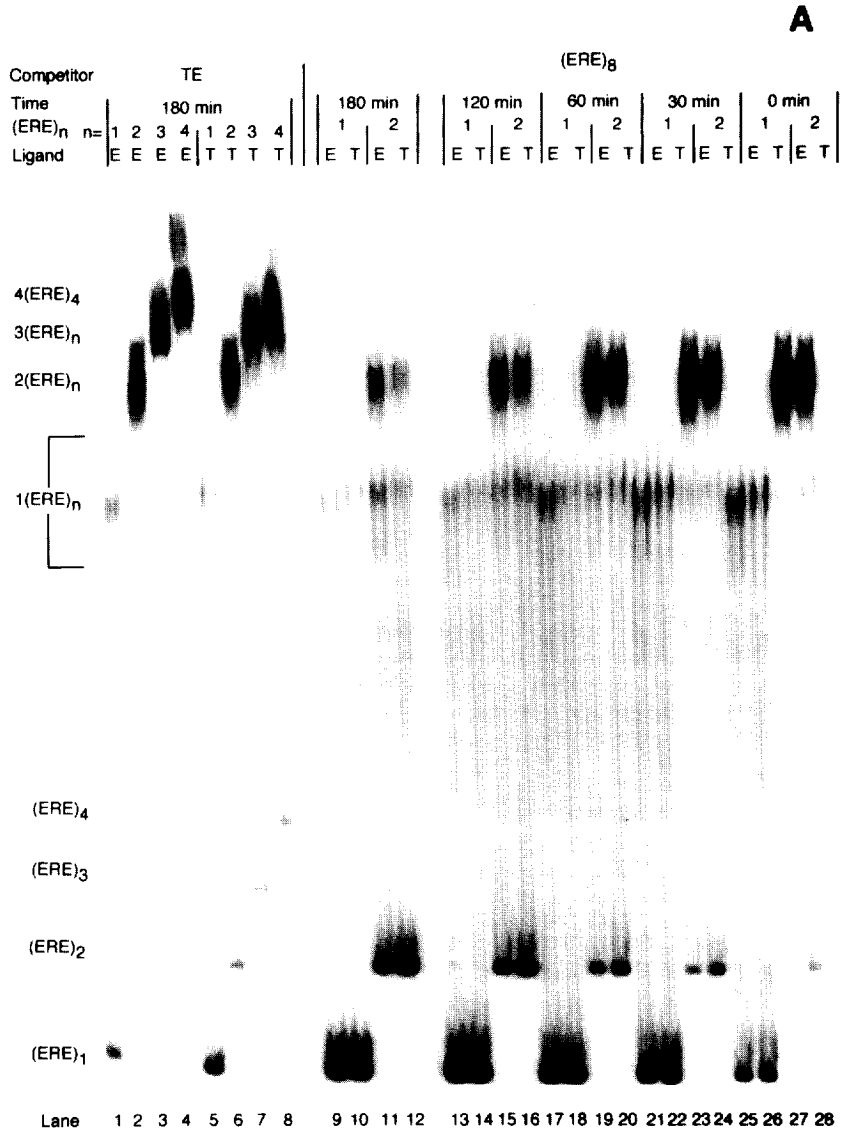

Fig. 4(A)—*caption overleaf*

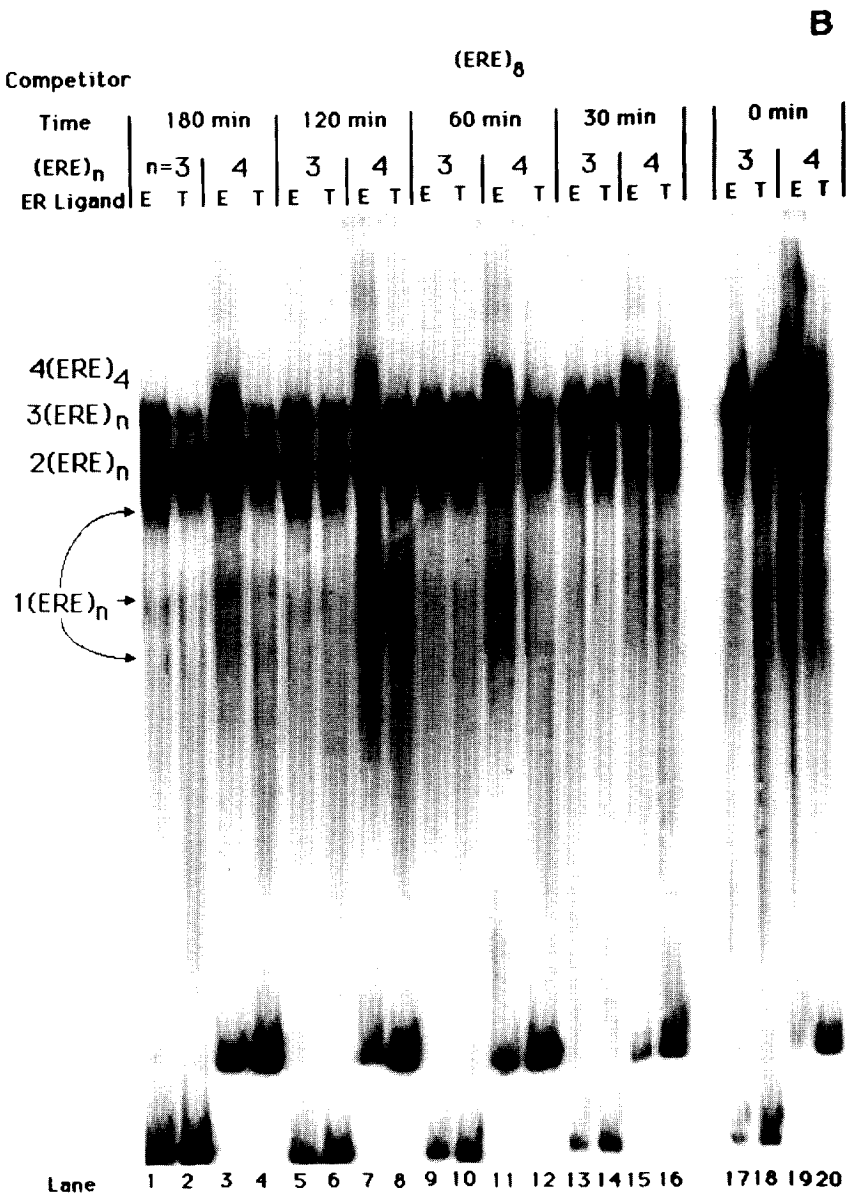

Fig. 4(B)

Fig. 4. Gel shift assay comparing dissociation of E_2–ER and 4-OHT–ER from $(ERE)_{1-4}$.Dissociation of E_2–ER and 4-OHT–ER from ERE was examined by gel shift assay. One hundred fmol E_2–ER (E) or 4-OHT–ER (T) was incubated with 20 fmol [^{32}P]ERE and 1.5 μg poly d(I–C) for 2.5 h at 4°C. Competitor (unlabeled $(ERE)_8$ or TE) was added for the indicated amount of time, and the samples were subjected to electrophoresis on a nondenaturing gel as described in Experimental. Shifted complexes containing [^{32}P]ERE are labeled at the upper left of the figures. Free [^{32}P]ERE appears in the band closest to the bottom of the figure in each lane. These gels are representative of three separate experiments giving identical results.

of [^{3}H] bound to the filter remained constant over the time course of each experiment, demonstrating that the aliquots applied to the filter contained the same input ER concentration. Specific [^{35}S]DNA bound at each time point was determined as in Experimental. The amount of time required for half of the specific [^{35}S]DNA counts to dissociate from ER bound to the filter ($t1/2$) was calculated.

The results of these experiments are summarized in Fig. 6. Side-by-side experiments measuring [^{3}H]4-OHT–ER and E_2–ER dissociation from $(ERE)_3$ and $(ERE)_4$ revealed a similar rate of decrease of [^{35}S]ERE retained by the filters. This shows that dissociation rate of 4-OHT–ER from $(ERE)_3$ and $(ERE)_4$ is not different from that of E_2–ER. Therefore, E_2–ER does not bind more tightly than 4-OHT–ER to $(ERE)_3$ and $(ERE)_4$. This finding is in agreement with the results of the DNase I footprint assay.

DISCUSSION

We applied quantitative DNase I footprinting to analyze how ER binds to multiple closely spaced EREs.

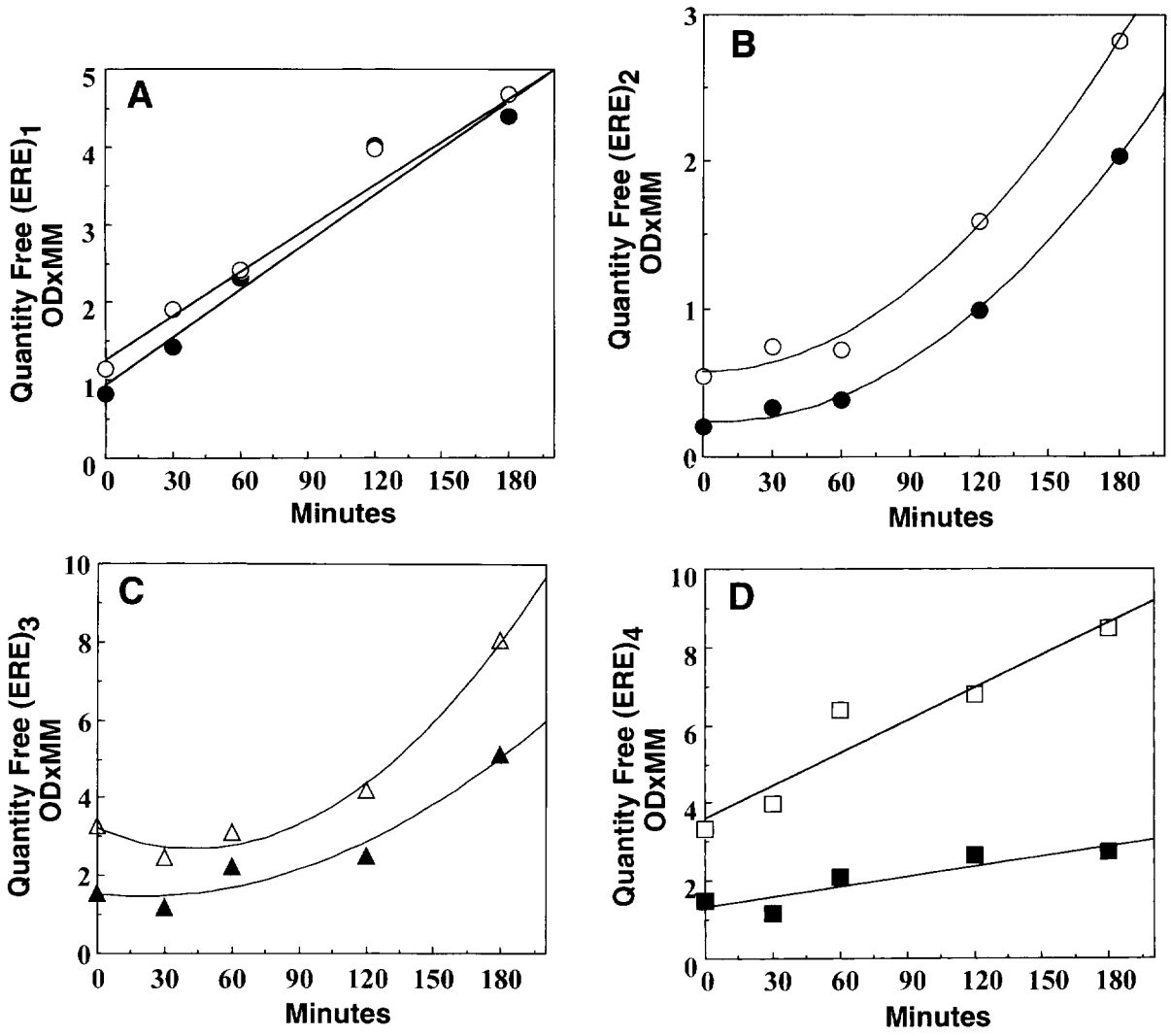

Fig. 5. Quantitation of free $(ERE)_{1-4}$ from Figs 4A and B. The quantity of free ERE at each time point in Figs 4A and B was determined by densitometric scanning as outlined in Experimental. Experiments containing 4-OHT–ER (open points) and E_2–ER (closed points) were graphed together for $(ERE)_{1-4}$. The lines were calculated using least squares regression analysis. The slopes of the lines represent the rate of appearance of free ERE.

This technique allowed us to identify regions protected from nuclease digestion by protein–DNA interaction, and calculate ER binding affinity for individual response elements located on the same DNA strand. These experiments showed that E_2–ER could bind EREs in constructs containing up to four tandem EREs with no change in E_2–ER–ERE affinity. We also examined the influence of ligand, location of a specific binding site with respect to other sites, and flanking sequences known to influence ER–ERE interaction, on the size, intensity, and position of the footprints.

ERE sequences protected by E_2–ER, 4-OHT–ER, TAz–ER, and unliganded ER were found to be identical. Several previous results suggested that 4-OHT–ER might adopt a conformation resulting in a larger footprint than E_2–ER. First, gel shift complexes containing 4-OHT–ER were similar to, but migrated slightly slower than those containing E_2–ER, implying larger 4-OHT–ER size. Second, using an equilibrium binding assay that detects ER–ERE interaction based on [^{3}H]liganded ER binding to [^{35}S]ERE DNA [25], we observed half the amount of 4-OHT–ER bound to $(ERE)_{1-4}$ at saturation when compared to E_2–ER [4]. E_2–ER binding to closely spaced EREs seemed to be more stable than to EREs spaced further apart, while the opposite result was detected for 4-OHT–ER [5]. One explanation for all of these observations may be that the 4-OHT–ER complex is larger than E_2–ER, and if so, the increased size of 4-OHT–ER was interfering with binding to closely spaced EREs. If this were true, 4-OHT–ER would protect a larger region of the ERE than E_2–ER. However, the footprints of E_2–ER and 4-OHT–ER were identical. It is possible that the apparent larger size of the 4-OHT–ER complex revealed by gel shift is the result of ligand-dependent

alterations in the overall conformation of the receptor [34] which do not alter the DNA binding domain.

Since the naturally occurring AT-rich region adjacent to the ERE increased the ERE binding affinity of both E_2–ER and 4-OHT–ER [5], we wanted to determine whether proteins present in our ER preparation bind to this region, or to other sequences proximal to the ERE. There was no DNase I protection of the sequences flanking the EREs. Although this indicates that other proteins do not stably interact with either the AT-rich region or with other sequences flanking the ERE, it is possible that lower affinity or transient binding events may take place in these regions. Such interactions may not be detected by DNase I protection assays. Interestingly, AT-rich regions between adjacent ERE sites became hypersensitive to DNase I digestion following ER binding. One possible explanation for the appearance of these hypersensitive sites is DNA bending. We suggested that one mechanism accounting for enhanced E_2–ER binding to an ERE flanked by an AT rich sequence may be intrinsic or induced DNA bending [5]. Specific nucleotide sequences, such as periodically repeated dA tracts, are intrinsically bent [reviewed in [35, 36]] and AT-rich sequences are characterized by low melting temperatures, DNA bending, and promotion of cruciform formation when adjacent to inverted repeat sequences [37]. ER–ERE binding has been shown to induce bending of the DNA adjacent to the ER [38–41]. Bent DNA may be more susceptible to DNase I cleavage, as the results here suggest. DNA bending may be important in ER-mediated transcriptional activation. Changes in chromatin structure may bring DNA binding sites, and their bound proteins, into closer proximity and recruit components of the transcription initiation complex.

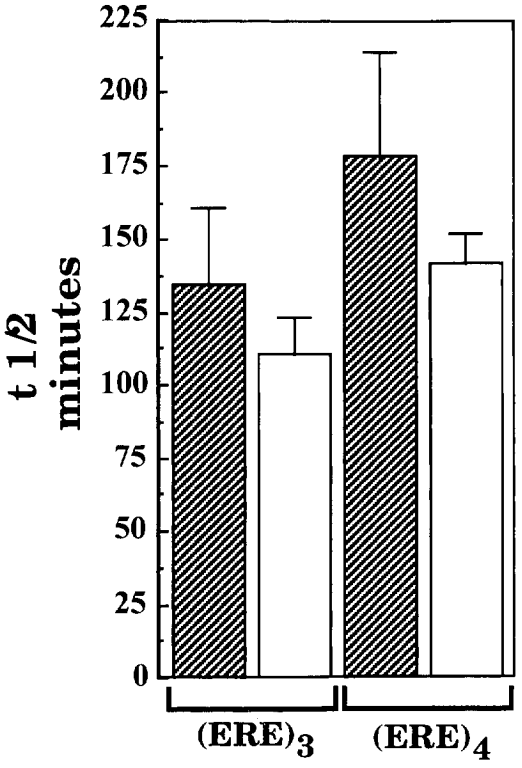

Fig. 6. Nitrocellulose filter dissociation assay comparing dissociation of 4-OHT–ER and E_2–ER from $(ERE)_3$ and $(ERE)_4$. E_2–ER (hatched bars) or 4-OHT–ER (white bars) was preincubated at 4°C with [^{35}S]plasmid with or without $(ERE)_{1-4}$ for 2.5 h. At time zero, 550-fold excess unlabeled plasmid DNA containing eight copies of the consensus ERE sequence $(ERE)_8$ was added as a competitor. The samples were incubated at 22°C for 3 h, allowing ER molecules that dissociated to be sequestered by the unlabeled competitor. Aliquots of the mixtures were removed at regular intervals over the 3 h and applied to nitrocellulose filters. Specific ER–ERE binding was followed over time as described in Experimental. Each bar represents the mean of at least three separate experiments. The error bars represent the standard error of the mean (SEM).

One question regarding the mechanisms of ER transactivation is the form of the ER that binds DNA. It is generally thought that ER binds DNA as a homodimer [reviewed in [42]], however, one report shows ER binding as a monomer or heterodimer [43]. If ER has the ability to bind ERE sites as a monomer, it should be able to recognize individual ERE half sites. We found no binding of ER to a single ERE half site ($(ERE)_{0.5}$), even at 20 nM receptor concentration (data not shown). The nuclear concentration of ER is thought to be about 10 nM in estrogen responsive cells [44]. However, there may be additional prerequisites in order for ER to associate with a half site. The effect of other natural proximal ERE elements may enhance ER interaction with half sites and variant EREs, such as the four tandem EREs that act synergistically to promote transcription of the chicken ovalbumin gene [45]. Also, ER may recognize ERE half sites in the context of other proximally bound transcription factors, or under conditions different from those used in our assay.

In previous work we regularly observed S-shaped binding curves and Hill coefficients greater than 1.5, indicative of cooperative binding of ER to adjacent EREs [4, 24, 5]. A simple explanation for the observed cooperativity is that ER–ER interactions stabilize binding to adjacent EREs. We predicted that the observed cooperative binding of E_2–ER to $(ERE)_3$ and $(ERE)_4$ would result in slower E_2–ER–ERE dissociation when compared to 4-OHT–ER, which appeared to bind non-cooperatively. However, this was not the case.

Nitrocellulose filter dissociation assays measured similar dissociation rates of E_2–ER and 4-OHT–ER from $(ERE)_3$ and $(ERE)_4$. Gel shift assays measured nearly identical dissociation rates for $(ERE)_1$, $(ERE)_2$ and $(ERE)_3$. However, 4-OHT–ER dissociated from $(ERE)_4$ at 2.6-fold the rate of E_2–ER. This small difference in dissociation rates differs from the results of both the nitrocellulose filter dissociation assay and the DNase I footprint assay, where similar E_2–ER and 4-OHT–ER kinetics were measured. The slightly slower E_2–ER dissociation rate measured by gel shift is probably not significant. It is likely that the gel shift assay conditions, with their unique hydrodynamic

properties and macromolecular concentrating effects, magnify a small difference in binding stability. Protein–DNA complexes with lifetimes as short as 1 min can be observed using gel shift assays that are run for several hours. Exchange reactions requiring dissociation of protein–DNA complexes can be slowed by two orders of magnitude in a gel, compared to free solution [46].

Interestingly, Scatchard analyses of our ER–ERE footprints produced curvilinear plots, indicative of cooperative binding (this alternative analysis of our data is not shown). Cooperative parameters should be interpreted in the light of equivalent binding affinity of ER to all sites on single or multiple EREs. One possibility is that at low concentrations, ER dimers may bind to non-adjacent ERE half sites in an array of tandem EREs, causing one ER dimer to occupy two ERE sites. ER binding to widely spaced half sites has been shown to be sufficiently stable to cause gene activation [47]. However, stability of such complexes is likely to be less than that of ER molecules fully saturating the array of EREs, and presumably all binding to adjacent half sites. This would cause a distortion of the binding curve at low ER concentration, producing an S-shape. This would not affect measurements of K_d, which are determined from the midpoint of the curve, which is minimally distorted.

In vivo, Ponglikitmongkol *et al.* found that ER did not appear to bind cooperatively to the consensus *Xenopus* vitellogenin A2 ERE [48]. In contrast, Martinez *et al.* [49] showed that cooperative binding of ER to two closely spaced imperfect EREs in the *Xenopus* vitellogenin B1 gene is responsible for the synergistic activation of reporter genes by this element. In gel mobility shift assays, a plasmid containing both *Xenopus* vitellogenin B1 EREs bound 4- to 8-fold more E_2–ER than the sum of the two plasmids containing each ERE alone [11]. Furthermore, the ER saturation binding curve for the construct containing both EREs was S-shaped, which suggested cooperativity. Martinez and Wali proposed that the synergy of reporter gene activation resulted from cooperative ER–ERE binding [49, 50]. These results, as well as ours, underscore the point that questions remain about the mechanistic interpretation of cooperative binding of ER to EREs. Further investigation is necessary to understand the nature of this complex phenomenon, and how it affects transcription.

An additional construct, ERE–AT to which E_2–ER binds cooperatively [5] was also examined. This construct contains two EREs, seven helical turns apart, flanked by AT-rich regions (Table 1). The orientation of these two EREs is identical to that of the first and third EREs in $(ERE)_3$, where the ER molecules bound to these sites may be in close proximity. DNase I footprinting revealed that ER bound ERE sites in ERE–AT with the same affinity as $(ERE)_1$.

Both 4-OHT–ER and TAz–ER showed ERE binding affinities similar to those determined for E_2–ER. Furthermore, unliganded, activated ER bound EREs with the same affinity as liganded ER. Similarly, Murdoch *et al.* [29] measured a dissociation constant of 0.45 nM for unliganded, heated rat uterine ER using an antibody-based assay. Experiments using human ER revealed that unliganded, E_2- 4-OHT- or ICI 164,384-liganded ER binds to EREs as a dimer *in vitro* [42]. Evidently, when ER is activated by heat or salt, the ligand does not regulate ER–ERE interactions. The question remains: how does ligand control the effects of ER on gene expression? The fact that ligand plays a role in gene expression is undisputed, yet the exact mechanisms through which it exerts its effects *in vivo* are unclear. Both ligand-dependent and ligand-independent ER–ERE binding have been reported *in vivo* [reviewed in [42]]. Early experiments indicated that ligand was required for ER–ERE complex formation in gel shift assays [50, 51]. However, recent re-evaluation of the construct used as a source of ER in this work found that it contained a mutation that altered the properties of the receptor, resulting in rapid heat inactivation [44, 52, 42]. In agreement with our results, others reported that ER binds EREs in the absence of hormone [22, 23, 53, 42] reviewed in [1]]. Recently, Zhuang *et al.* [54] used a promoter interference assay to compare the ability of non-hormone binding ER mutants and wild type ER to bind EREs. They found that both wild type and unliganded ER mutants bound EREs in a similar fashion *in vivo*. Furthermore, the mutants were able to repress wild type ER activity when coexpressed. Their results support the idea that unliganded ER is free to dimerize and bind ERE sequences *in vivo*. Interestingly, however, binding of *Xenopus* ER to ERE reporter constructs was found to be estrogen dependent [55].

Unliganded ER may be present as a homodimer in the nucleus, able to bind available ERE elements, but unable to promote transcription. Ligand binding changes the conformation of regions of the receptor that affect ER interactions with components of the transcription initiation complex. These components may include proteins which bind the ligand binding domain of ER when liganded with E_2, but not when liganded with antiestrogens [56, 57]. In this model, ER–ERE binding is a step that is necessary, but not sufficient, for transcriptional activation. Binding of ligand, either before or after ER–ERE binding, determines the transcriptional activity of ER.

In summary, the use of a quantitative DNase I footprinting assay [28] that does not disturb the ER–ERE binding equilibrium, allowed for the first time, direct measurement of the affinity of ER binding to each ERE within the context of multiple tandem EREs. We demonstrated that activated ER, whether unliganded or liganded by E_2, 4-OHT, or TAz binds with equal high affinity to single or multiple tandem consensus EREs, but not to an ERE half site. This

supports the hypothesis that ER transactivation *in vivo* results not from enhanced ER binding to EREs in response to ligand, but from ligand induced changes in receptor conformation that facilitate ER interaction with other proteins required for increased transcriptional efficiency. Moreover, these results indicate that cooperative ER–ERE binding, as measured previously [1, 4, 5, 24] does not result from direct interactions between ER dimers that increase ER–ERE binding affinity, but could be attributed to the binding of single ER dimers to multiple nonadjacent ERE half sites. The ER dimer, liganded or unliganded, protected an identical 22 bp stretch of DNA centered on the inverted repeat. Interestingly, the AT-rich region flanking the consensus ERE, which increased ER–ERE binding affinity [5], was not protected from DNase I digestion, but was rendered hypersensitive to nuclease digestion by ER binding. This finding suggests that the region is bent, possibly expediting chromatin changes required for transcriptional activation.

REFERENCES

1. Klinge C.M., Bambara R.A. and Hilf R. (1992) What differentiates antiestrogen-liganded versus estradiol-liganded estrogen receptor action? *Oncology Res.* **4,** 137–144.
2. Parker M. G. and Bakker O.: Nuclear hormone receptors: concluding remarks. In: *Nuclear Hormone Receptors* (Edited by M. Parker). Academic Press, New York (1991) 377–395.
3. Gronemeyer H. (1993) Transcription activation by nuclear receptors. *J. Receptor Res.* **13,** 667–691.
4. Klinge C.M., Bambara R.A. and Hilf R. (1992) Antiestrogen liganded estrogen receptor interaction with estrogen responsive element DNA *in vitro*. *J. Steroid Biochem. Molec. Biol.* **43,** 249–262.
5. Anolik J.H., Klinge C.M., Hilf R. and Bambara R.A. (1995) Cooperative binding of estrogen receptor to DNA depends on spacing of binding sites, flanking sequence, and ligand. *Biochemistry* **34,** 2511–2520.
6. Tsai S.Y., Tsai M.A. and O'Malley B.W. (1989) Cooperative binding of steroid hormone receptors contributes to transcriptional synergism at target enhancer elements. *Cell* **57,** 443–448.
7. Poellinger L., Yoza B.K. and Roeder R.G. (1989) Functional cooperativity between protein molecules bound at two distinct sequence elements of the immunoglobulin heavy-chain promoter. *Nature* **337,** 573–576.
8. Schmid W., Strahle U., Schutz G., Schmitt J. and Stunnenberg H. (1989) Glucocorticoid receptor binds cooperatively to adjacent recognition sites. *EMBO J.* **8,** 2257–2263.
9. Davidson I., Xiao J.H., Rosales R., Staub A. and Chambon R. (1988) The HeLa cell protein TEF-1 binds specifically and cooperatively to two SV40 enhancer motifs of unrelated sequence. *Cell* **54,** 931–942.
10. LeBowitz J.H., Clere R.G., Brenowitz M. and Sharp P. (1989) The Oct-2 protein binds cooperatively to adjacent octamer sites. *Genes Dev.* **3,** 1625–1638.
11. Martinez E. and Wahli W. (1989) Cooperative binding of estrogen receptor to imperfect estrogen-responsive DNA elements correlates with their synergistic hormone-dependent enhancer activity. *EMBO J.* **8,** 3781–3791.
12. Hochschild A. and Ptashne M. (1986) Homologous interactions of lambda repressor and lambda Cro with the lambda operator. *Cell* **44,** 681–687.
13. Lerner L.J. and Jordan V.C. (1990) Development of antiestrogens and their use in breast cancer: Eighth Cain Memorial Lecture. *Cancer Res.* **50,** 4177–4189.
14. Jordan V.C. (1984) Biochemical pharmacology of antiestrogen action. *Pharmac. Rev.* **36,** 245–276.
15. Katzenellenbogen B.S., Norman M.J., Eckert R.L., Peltz S.W. and Mangel W.F. (1984) Bioactivities, estrogen receptor interactions, and plasminogen activator-inducing activities of tamoxifen and hydroxy-tamoxifen isomers in MCF-7 human breast cancer cells. *Cancer Res.* **44,** 112–119.
16. Harlow K.W., Smith D.N., Katzenellenbogen J.A., Green G.A. and Katzenellenbogen B.S. (1989) Identification of cysteine, 530 as the covalent attachment site of an affinity-labeling estrogen (ketononestrol aziridine)and antiestrogen (tamoxifen aziridine) in the human estrogen receptor. *J. Biol. Chem.* **264,** 17476–17485.
17. Danielian P.S., White R., Hoare S.A., Fawell S.E. and Parker M.G. (1993) Identification of residues in the estrogen receptor that confer differential sensitivity to estrogen and hydroxytamoxifen. *Molec. Endocr.* **7,** 232–240.
18. Robertson D.W., Wei L.L., Hayes J.R., Carlson K.E., Katzenellenbogen J.A. and Katzenellenbogen B.S. (1981) Tamoxifen aziridines: effective inactivators of the estrogen receptor. *Endocrinology* **109,** 1298–1300.
19. Hansen J.C. and Gorski J. (1986) Conformational transitions of the estrogen receptor monomer. Effects of estrogens, antiestrogen, and temperature. *J. Biol. Chem.* **261,** 13990–13996.
20. Giambiagi N. and Pasqualini J.R. (1988) Immunological differences between the estradiol-, tamoxifen- and 4-hydroxytamoxifen- estrogen receptor complexes detected by two monoclonal antibodies. *J. Steroid Biochem.* **30,** 213–217.
21. Ruh M.F., Turner J.W., Paulson C.M. and Ruh T.S. (1990) Differences in the form of the salt transformed estrogen receptor when bound by estrogen versus antiestrogen. *J. Steroid Biochem.* **36,** 509–516.
22. Lees J.A., Fawell S.E. and Parker M.G. (1989) Identification of constitutive and steroid-dependent transactivation domains in the mouse oestrogen receptor. *J. Steroid Biochem.* **34,** 33–39.
23. Brown M. and Sharp P.A. (1990) Human estrogen receptor forms multiple protein-DNA complexes. *J. Biol. Chem.* **265,** 11238–11243.
24. Klinge C.M., Peale F.V., Hilf R., Bambara R.A. and Zain S. (1992) Cooperative estrogen receptor interaction with consensus or variant estrogen response elements *in vitro*. *Cancer Res.* **52,** 1073–1081.
25. Ludwig L.B., Klinge C.M., Peale F.V., Jr., Bambara R.A., Zain S. and Hilf R. (1990) A microtiter well assay for quantitave measurement of estrogen receptor binding to estrogen-responsive elements. *Molec. Endocr.* **4,** 1027–1033.
26. Peale F.V., Jr., Ishibe Y., Klinge C.M., Zain S., Hilf R. and Bambara R.A. (1989) Rapid purification of the estrogen receptor by sequencespecific DNA affinity chromatography. *Biochemistry* **28,** 8671–8675.
27. Sambrook J., Fritsch E. F. and Maniatis T.: *Molecular Cloning,* Second Edition. Cold Spring Harbor Laboratory Press, New York (1989).
28. Brenowitz M., Senear D.F., Shea M.A. and Ackers G.K. (1986) 'Footprint' titrations yield valid thermodynamic isotherms. *Proc. Natl. Acad. Sci. U.S.A.* **83,** 8462–8466.
29. Murdoch F.E., Meier D.A., Furlow D.F., Grunwald K.A.A. and Gorski J. (1990) Estrogen receptor binding to a DNA response element *in vitro* is not dependent upon estradiol. *Biochemistry* **29,** 8377–8385.
30. Curtis S. and Korach K. (1990) Uterine estrogen receptor interaction with estrogen-responsive DNA sequences *in vitro*: effects of ligand binding on receptor-DNA complexes. *Molec. Endocr.* **4,** 276–286.
31. Landel C.C., Kushner P.J. and Greene G.L. (1994) The interaction of human estrogen receptor with DNA is modulated by receptor associated proteins. *Molec. Endocr.* **8,** 1407–1419.
32. Greene G.L. and Press M.F. (1986) Structure and dynamics of the estrogen receptor. *J. Steroid Biochem.* **24,** 1–7.
33. Ausubel M. ed.: *Current Protocols in Molecular Biology*, Vols 1 and 2, Suppl. 8. Greene Pub. Assoc. and Wiley Interscience, New York (1987).
34. Fritsch M., Leary C.M., Furlow J.D., Ahrens H., Schuh T.J., Mueller G.C. and Gorski J. (1992) A ligand induced conformational change in the estrogen receptor is localized in the steroid binding domain. *Biochemistry* **31,** 5303–5311.
35. Bracco L., Kotlarz D., Kolb A., Diekniann S. and Buc H. (1989) Synthetic curved DNA sequences can act as transcriptional activators in *Escherichia coli*. *EMBO J.* **8,** 4289–4296.

36. Giese K., Cox J. and Grosschedl R. (1992) The HMG domain of lymphoid enhancer factor 1 binds DNA and facilitates assembly of functional nucleoprotein structures. *Cell* **69,** 185–195.
37. Wang Y. and Sauerbier W. (1989) Flanking AT-rich sequences may lower the activation energy of cruciform extrusion in supercoiled DNA. *Biochem. Biophys. Res. Commun.* **158,** 423–431.
38. Sabbah M., Le Ricousse S., Redeuilli G. and Baulieu E.E. (1992) Estrogen receptor-induced bending of the *Xenopus* vitellogenin A2 gene hormone response element. *Biochem. Biophys. Res. Commun.* **185,** 944–952.
39. Nardulli A.M. and Shapiro D.J. (1992) Binding of the estrogen receptor DNA binding domain to the estrogen response element induces DNA bending. *Molec. Cell. Biol.* **12,** 2037–2042.
40. Nardulli A.M., Greene G.L. and Shapiro D.J. (1993) Human estrogen receptor bound to an estrogen response element bends DNA. *Molec. Endocr.* **7,** 331–340.
41. Nardulli A.M., Grobner C. and Cotter D. (1995) Estrogen receptor-induced DNA bending: orientation of the bend and replacement of an estrogen response element with an intrinsic DNA bending sequence. *Molec. Endocr.* **9,** 1064–1076.
42. Metzger D., Berry M., Ali S. and Chambon P. (1995) Effect of antagonists on DNA binding properties of the human estrogen receptor *in vitro* and *in vivo*. *Molec. Endocr.* **9,** 579–591.
43. Furlow J.D., Murdoch F.E. and Gorski J. (1993) High affinity binding of the estrogen receptor to a DNA response element does not require homodimer formation or estrogen. *J. Biol. Chem.* **268,** 12519–12525.
44. Gorski J., Furlow J.D., Murdoch F.E., Fritsch M., Kaneko K., Ying C. and Malayer J. (1993) Perturbations in the model of estrogen receptor regulation of gene expression. *Biology of Reproduction* **48,** 8–14.
45. Kato S., Tora L., Yamauchi J., Masushige S., Bellard M. and Chambon P. (1992) A far upstream estrogen response element of the ovalbumin gene contains several half-palindromic 5'-TGACC-3'motifs acting synergistically. *Cell* **68,** 731–742.
46. Fried M. and Crothers D.M. (1981) Equilibria and kinetics of lac repressor-operator interactions by polyacrylamide gel electrophoresis. *Nucl. Acids Res.* **9,** 6505–6524.
47. Kato S., Haruna S., Suzawa M., Shoichi M., Tora L., Chambon P. and Gronemeyer H. (1995) Widely spaced, directly repeated PuGGTCA elements act as promiscuous enhancers for different classes of nuclear receptors. *Molec. Cell. Biol.* **15,** 5858–5867.
48. Pongilikitmongkol N., White J.H. and Chambon P. (1990) Synergistic activation of transcription by the human estrogen receptor bound to tandem responsive elements. *EMBO J.* **9,** 2221–2231.
49. Martinez E., Givel F. and Wahli W. (1987) The estrogen responsive element as an inducible enhancer: DNA sequence requirements and conversion to a glucocorticoid-responsive element.. *EMBO J.* **6,** 3719–3727.
50. Kumar V., Green S., Staub A. and Chambon P. (1986) Localisation of the oestradiol-binding and putative DNA-binding domains of the human oestrogen receptor. *EMBO J.* **5,** 2231–2236.
51. Theulaz I., Hipskind R., Heggler-Bordier B., Green S., Kumar V., Chambon P. and Wahli W. (1988) Expression of human estrogen receptor mutants in *Xenopus* oocytes: correlation between transcriptional activity and ability to form protein-DNA complexes. *EMBO J.* **7,** 1653–1660.
52. Gronemeyer H. (1991) Transcription activation by estrogen and progesterone receptors. *Ann. Rev. Genet.* **25,** 89–123.
53. Reese J.C. and Katzenellenbogen B.S. (1991) Differential DNA binding abilities of estrogen receptor occupied with two classes of antiestrogens: studies using human receptor overexpressed in mammalian cells. *Nucl. Acids Res.* **19,** 6595–6602.
54. Zhuang Y., Katzenellenbogen B.S. and Shapiro D.J. (1995) Estrogen receptor mutants which do not bind 17β-estradiol dimerize and bind to the estrogen response element *in vivo*. *Molec. Endocr.* **9,** 457–466.
55. Xing H. and Shapiro D.J. (1993) An estrogen receptor mutant exhibiting hormone-independent transactivation an enhanced affinity for the estrogen response element. *J. Biol. Chem.* **268,** 23227–23233.
56. Halachmi S., Marden E., Martin G., MacKay H., Abbondanza C. and Brown M. (1994) Estrogen receptor-associated proteins: possible mediators of hormone-induced transcription. *Science* **264,** 1455–1458.
57. Cavailles V., Dauvois P.S., Danielian P.S. and Parker M.G. (1994) Interaction of proteins with transcriptionally active estrogen receptors. *Proc. Natl. Acad. Sci. U.S.A.* **91,** 10009–100013.